

VI. GASEOUS ELECTRONICS*

Academic and Research Staff

Prof. G. Bekefi
Prof. W. P. Allis

Prof. S. C. Brown
Prof. B. L. Wright
Dr. E. V. George

J. J. McCarthy
W. J. Mulligan

Graduate Students

S. F. Fulghym, Jr.
L. D. Pleasance
G. Raff

A. TIME-DEPENDENT THRESHOLD CHARACTERISTICS OF PULSED NOBLE ION LASERS

Study of the time-dependent characteristics of the laser output from pulsed Xenon and Argon discharges continues. The 5145 Å Ar II transition was found to exhibit laser pulse delay characteristics similar to those of the Xenon lines previously reported.¹ Figure VI-1 illustrates a delay time of 28 μs between the initiation of the excitation current pulse (upper trace) and the start of the laser pulse (lower trace) for the 5145 Å line. With increasing values of peak current, the time delay to onset of laser oscillation is observed to decrease, as is shown in Fig. VI-2 for two pressures of Argon, again at the 5145 Å transition.

Figure VI-3 shows the relevant energy levels in singly ionized Argon for both the 5145 Å and 4880 Å lines. It is seen that the two lines share a common lower level which, in turn, depopulates via an extremely fast ($\tau=0.4$ ns) vacuum ultraviolet radiative transition to the ion ground state. Under the assumption that this ultraviolet radiation is not significantly trapped, the time-dependent characteristics of the 5145 Å line, to a good approximation, can be expected to involve only the population processes of its upper level, principally the spontaneous decay rate and the electron-ion destructive collision cross section. The lack of delay phenomena in the 4880 Å transition throughout the ranges of pressure and current in which the 5145 Å characteristics are exhibited, indicates that the assumption of negligible trapping is justified. To verify these assumptions regarding the shared lower level, we plan to insert a Littrow prism in place of one of the end reflectors so that the 4880 Å laser line is suppressed. Further information will be obtained from planned measurements of the spontaneous emission of the Argon transitions that terminate on the $4s^2P_{3/2}$ level.

Spontaneous emission measurements were taken of several ionized Xenon lines. In general, the time relationship between current pulse and laser seems to be upheld

*This work was supported by the Joint Services Electronics Programs (U. S. Army, U. S. Navy, and U. S. Air Force) under Contract DA 28-043-AMC-02536(E).

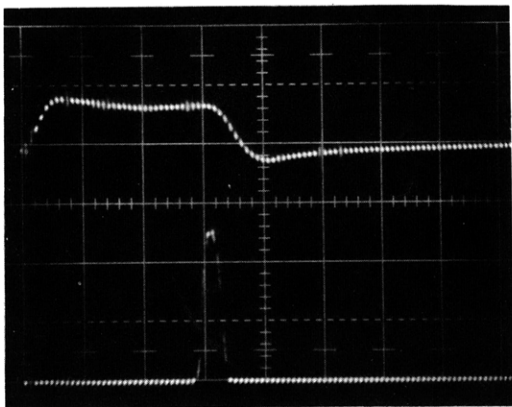


Fig. VI-1.

The 5145 Å laser line of Ar II; pressure = 30 mTorr. Upper trace: current pulse, 10 A/div.

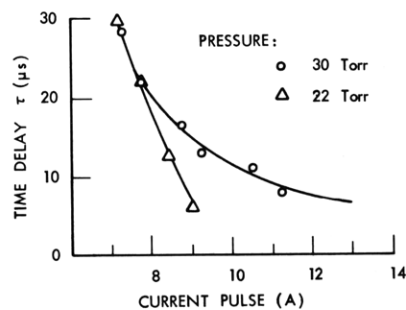


Fig. VI-2.

Time delay τ as a function of peak discharge current I for the

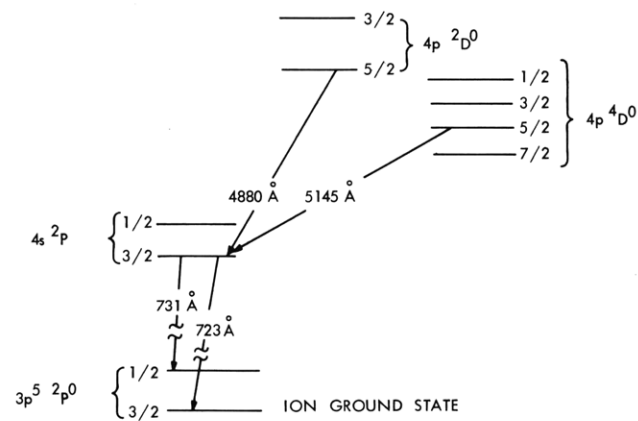


Fig. VI-3.

Partial energy level diagram for singly ionized Argon.

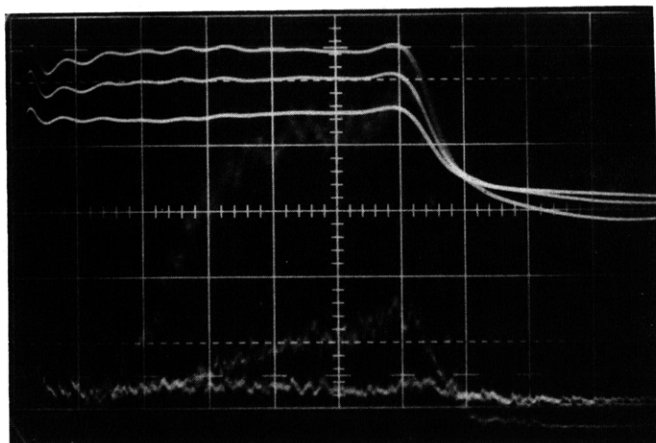
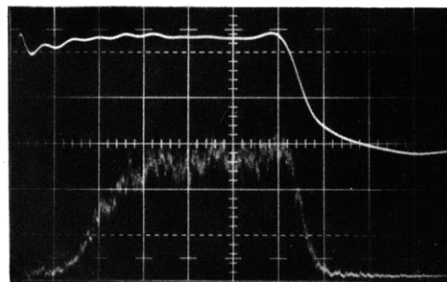
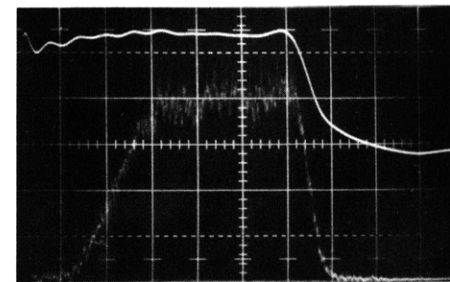


Fig. VI-4. Upper trace: current pulses, 20 A/div. Lower trace: spontaneous emission of the 4954 Å Xe III line at 30 mTorr pressure, 10 mV/div. The order of the emission traces from bottom to top corresponds to the order of the current traces.



(a)



(b)

Fig. VI-5. Upper trace: current pulse, 20 A/div. Lower trace: spontaneous emission, of the 4954 Å Xe III line at 30 mTorr pressure, during laser oscillation. (b) Same as (a), except that laser oscillation is prevented.

between the current pulse and the spontaneous emission: that is, delays between current pulse and emission occur for lines that show time-dependent laser characteristics, and do not occur for lines showing no laser delays. Figure VI-4 illustrates the spontaneous emission of the 4950 Å Xe III line as detected through the wall of the plasma tube, for 3 values of discharge current. Figure VI-5 compares the emission of the same Xenon line when laser oscillation is allowed (a), and when it is prevented (b). These Xenon data are now being analyzed.

G. Raff, S. F. Fulghum, Jr., E. V. George

References

1. E. V. George and S. F. Fulghum, Jr., "Time-Dependent Threshold Characteristics of a Pulsed Xenon Laser," Quarterly Progress Report No. 96, Research Laboratory of Electronics, M. I. T., January 15, 1970, pp. 113-115.

B. MICROWAVE DIAGNOSTICS OF HIGH-DENSITY LASER PLASMAS

An investigation of the properties of ion laser discharges by means of microwave cavity techniques has begun. Electron densities of 10^{13} cm⁻³ or higher are required for the operation of these lasers. The discharge current necessary to achieve these high densities is held to a minimum by restricting the discharge to a column of a few millimeters diameter. Considerable experimental information is available on the relationship of a laser output to gross discharge parameters, such as discharge current, voltage, and gas pressure. Much less information is available on its relationship to the plasma parameters of such discharges. The predictions of various theoretical models of the excitation mechanism for ion lasers are strongly dependent on these plasma properties. In particular, the interpretation of power output saturation with increasing current density depends critically on the assumed relationship between the current density and electron density. It has been shown¹ that the TE₀₁₁ mode may be used to probe high-density plasmas. The perturbation expansion used for calculating the expected frequency shift breaks down for $\omega_p^2/\omega^2 \sim 10$. The analysis described below removes this restriction by considering the detailed variation of the fields in the plasma.

The electric field of the TE₀₁₁ mode is azimuthal and satisfies the equation

$$\frac{1}{r} \frac{\partial}{\partial r} r \frac{\partial}{\partial r} E_{\theta} + \left(\frac{\omega^2}{c^2} \epsilon - k^2 \right) E_{\theta} = 0, \quad (1)$$

where $\epsilon = 1 - \omega_p^2/\omega^2$, and $k = \pi/\ell$ is the axial wave number.

The radial variation of E_{θ} is shown in Fig. VI-6. For $\omega_p/\omega > 1$ the field decays into the plasma with a characteristic length $\delta = c/\omega_p$. The resonant frequency, ω , of the

(VI. GASEOUS ELECTRONICS)

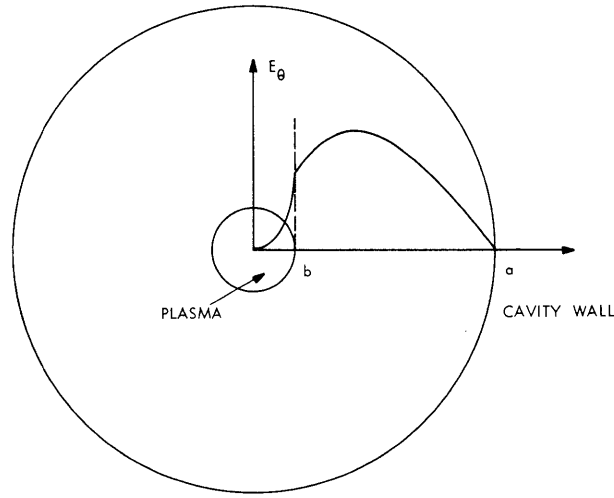


Fig. VI-6. Radial variation of the electric field of the TE_{011} mode in the presence of a plasma.

mode is determined by the boundary conditions at the cavity wall ($E_\theta = 0$) and at the edge of the plasma (continuity of E_θ and its radial derivative). The resulting equation for ω may be written

$$f = g(\omega) - h(\omega, \omega_p) = 0, \quad (2)$$

where $h(\omega, \omega_p)$ is a function of the fields in the plasma, and $g(\omega)$ is a function of the fields between the plasma and the cavity wall. For a uniform plasma

$$h(\omega, \omega_p) = \frac{I_1(qb)}{qI_0(qb)} \quad (3)$$

and

$$g(\omega) = \frac{J_1(pb)Y_1(pa) - J_1(pa)Y_1(pb)}{p(J_0(pb)Y_1(pa) + J_1(pa)Y_0(pb))} \quad (4)$$

where $p^2 = \frac{\omega^2}{c^2} - k^2$ and $q^2 = \frac{\omega_p^2}{c^2} + k^2 - \frac{\omega^2}{c^2} \gg 1$. The resonant frequency calculated for this model is shown in Fig. VI-7 as a function of ω_p^2/ω^2 . The resonant frequency in the absence of plasma is ω_0 . As ω_p^2/ω^2 increases, the fields are excluded from the plasma and the resonant frequency approaches a limit, ω_m , which corresponds to a metal post in the cavity.

In principle the curve plotted in Fig. VI-7 could be used to convert measured frequency shifts into electron density. In practice, however, two further problems must

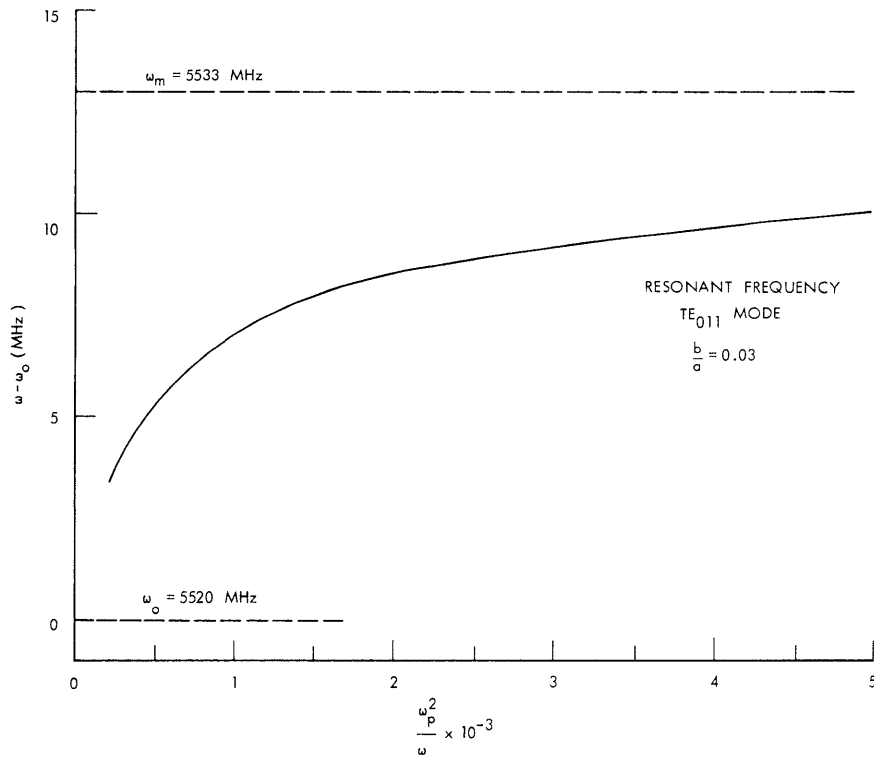


Fig. VI-7. Resonant frequency of the TE_{011} mode as a function of ω_p^2/ω^2 for a uniform plasma.

be considered. First, the fields used to generate Eq. 4 are modified by the presence of the discharge tube. Usually such effects are neglected, but in the experiments considered here the volume of the cavity occupied by the cooling liquid and discharge tube is much larger than that of the plasma. While it is possible to correct Eq. 4 rigorously for the effect of the discharge tube, the following approximate approach is much simpler. The function f may be expanded in a Taylor series about the frequency ω_m at which $g(\omega_m) = 0$ to give

$$(\omega - \omega_m) = \frac{h(\omega_m, \omega_p)}{\frac{\partial g(\omega_m)}{\partial \omega} - \frac{\partial h(\omega_m, \omega_p)}{\partial \omega}}. \quad (5)$$

For $(\omega_m - \omega_0)/\omega_m \ll 1$ the derivative involving the fields outside the plasma may be approximated by $\frac{\partial g(\omega_m)}{\partial \omega} \approx \frac{-h(\omega_0, 0)}{\omega_m - \omega_0}$ to yield

$$(\omega - \omega_m) = \frac{-h(\omega_m, \omega_p)}{\frac{h(\omega_0, 0)}{\omega_m - \omega_0} + \frac{\partial h(\omega_m, \omega_p)}{\partial \omega}}. \quad (6)$$

(VI. GASEOUS ELECTRONICS)

Equation 6 expresses the frequency shift in terms of the fields in the plasma and a single measurable parameter, $\omega_m - \omega_o$, representing the fields outside the plasma. The frequency shift calculated with Eqs. 3 and 6 agrees with the exact solution shown in Fig. VI-7, provided the calculated value of $(\omega_m - \omega_o)$ is used. Unfortunately, (6) cannot be expressed as a universal curve and must be solved for each experimental geometry.

A second consideration is the effect of radial density gradients on the fields inside the plasma. Since the fields decay inward from the plasma edge with a characteristic length $\delta = c/\omega_p$, deviations should be expected for $\omega_p^2/\omega^2 > c^2/\omega^2 b^2$. For the dimensions in this experiment this gives $\omega_p^2/\omega^2 \sim 200$. Rigorous calculations of $h(\omega, \omega_p)$ for a parabolic density distribution shows, however, that for the condition given above the frequency shift differs by less than 10% from the corresponding uniform density case at the same central density. This is not unexpected, since the fields in the plasma are determined mainly by the high-density regions. While additional calculations are being made to confirm this result, it is felt that calculations using (3) and (6) can be used with reasonable accuracy up to $\omega_p^2/\omega^2 \sim 1000$.

Preliminary experimental measurements have been made on the Argon-ion laser shown schematically in Fig. VI-8. The demountable discharge tube is a 2 mm ID quartz capillary with 12 mm OD cooling jacket. The tube is cooled by a liquid (Dow Corning

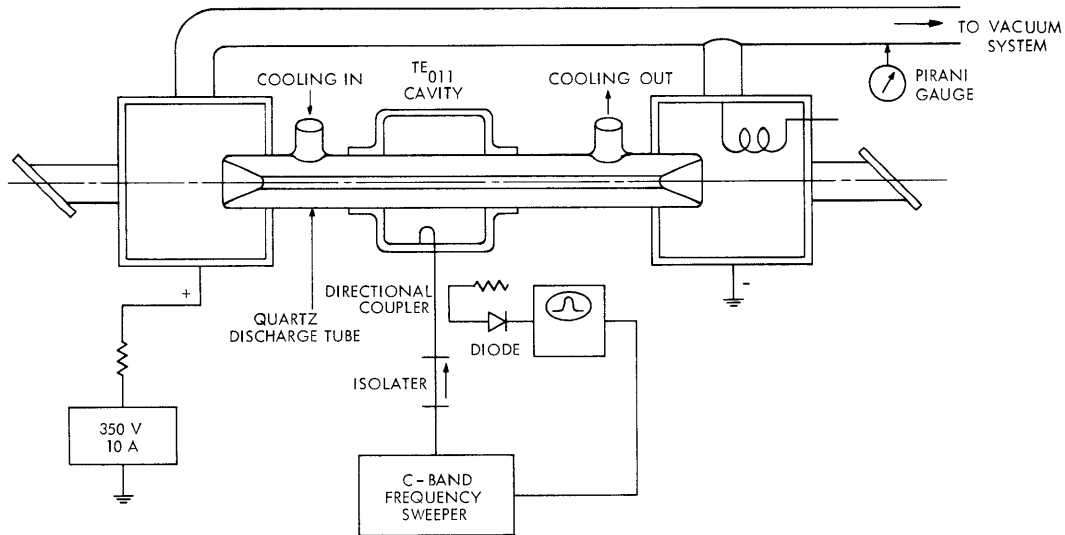


Fig. VI-8. Experimental system.

silicone fluid) having low losses at microwave frequencies. The active length of the discharge is 40 cm. The microwave cavity is 7.8 cm in diameter and 5.4 cm long. The TE₀₁₁ mode is excited by a loop at a frequency of 5475 MHz with the discharge tube in the cavity but without a plasma. The frequency shift associated with a metal post the

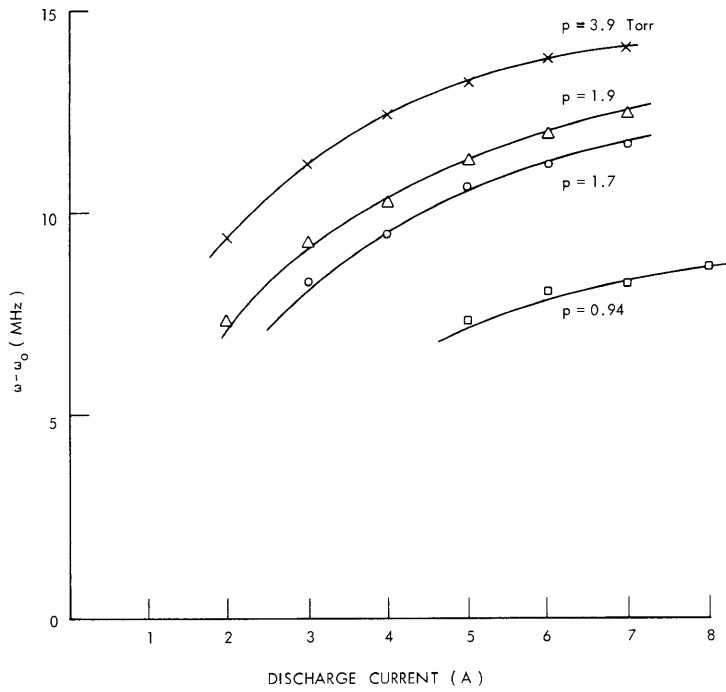


Fig. VI-9.

Frequency shift as a function of discharge current in the Argon laser.

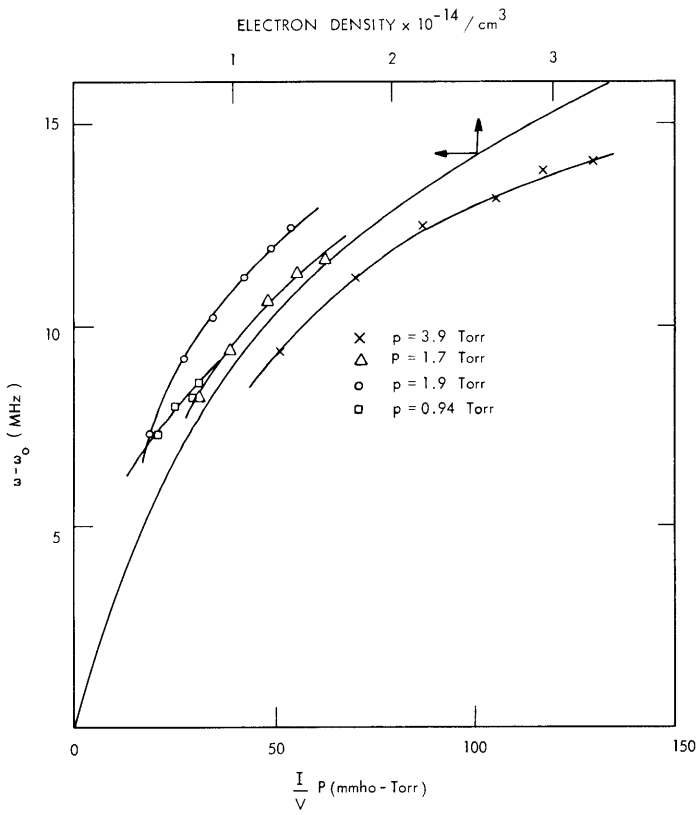


Fig. VI-10.

Measured and predicted frequency shift for a model based on electron neutral collisions.

(VI. GASEOUS ELECTRONICS)

size of the plasma is found to be 27.5 MHz. This is accomplished by filling the discharge tube with mercury.

The resonant frequency of the cavity was measured as a function of discharge current for several pressures. The voltage drop across the discharge tube was also recorded. Pressures were measured with a Pirani gauge. The measured frequency shifts are shown in Fig. VI-9. If the discharge is dominated by electron neutral collisions, the electron density is related to the discharge parameters by the expression

$$\omega_p^2 = \beta p \frac{I}{V}, \quad (7)$$

where β is a constant determined by the geometry and electron temperature, and p is the pressure. The electric field in the plasma has been taken to be proportional to the total voltage drop across the discharge. The data of Fig. VI-9, renormalized to test Eq. 7 is shown in Fig. VI-10. Also shown is the calculated relationship between the frequency shift and electron density. This curve was adjusted to fit a single point. The adjustable parameter is the constant β in (7). The value of β taken from Fig. VI-10 was found to be consistent with an electron temperature of a few electron volts. The displacement of the curves probably results from inaccuracies in the measurements of the pressure.

The main conclusion reached thus far is that it is possible to measure electron densities in the range found in ion lasers using microwave cavities. The preliminary data show no gross deviation from the behavior expected for a discharge dominated by electron neutral collisions.

L. D. Pleasance, E. V. George

References

1. S. J. Buchsbaum and S. C. Brown, Phys. Rev. 106, 196 (1957).